GREAVES, C. (1985). *J. Appl. Cryst.* **18**, 48-50.
GREAVES, C., THOMAS, M. A. & TURNER, M. (1983). *Power Sources*, **9**, 163-182.
HEWAT, A. W. (1979). *Acta Cryst.* A**35**, 248.
HEWAT, A. W. & BAILEY, I. (1976). *Nucl. Instrum. Methods*, **137**, 463-471.
JOHNSON, C. K. (1965). *ORTEP*. Report ORNL-3794, Oak Ridge National Laboratory, Tennessee.
KOBER, F. P. (1965). *J. Electrochem. Soc.* **112**, 1064-1067.
KOBER, F. P. (1967). *J. Electrochem. Soc.* **114**, 215-218.
MCEWEN, R. S. (1971). *J. Phys. Chem.* **75**, 1782-1789.
OLIVA, P., LEONARDI, J., LAURENT, J. F., DELMAS, C., BRACONNIER, J. J., FIGLARZ, M., FIEVET, F. & DE GUIBERT, A. (1982). *J. Power Sources*, **8**, 229-255.
PETERSON, R. C., HILL, R. J. & GIBBS, G. V. (1979). *Can. Mineral.* **17**, 703-711.
RIETVELD, H. M. (1967). *Acta Cryst.* **22**, 151-152.
RIETVELD, H. M. (1969). *J. Appl. Cryst.* **2**, 65-71.
SAKASHITA, M. & SATO, N. (1973). *Bull. Chem. Soc. Jpn*, **46**, 1983-1987.
SZYTULA, A., MURASIK, A. & BALANDA, M. (1971). *Phys. Status Solidi B*, **43**, 125-128.
TUOMI, D. (1965). *J. Electrochem. Soc.* **112**, 1-12.
WENGELER, H., MARTENS, R. & FREUND, F. (1980). *Ber. Bunsenges. Phys. Chem.* **84**, 873-880.
YOUNG, R. A. & WILES, D. B. (1982). *J. Appl. Cryst.* **15**, 430-438.
ZIGAN, F. & ROTHBAUER, R. (1967). *Neues Jahrb. Mineral. Monatsh.* pp. 137-143.

Acta Cryst. (1986). B**42**, 55-58

Cuboctahedral Anion Clusters in Fluorite-Related Superstructures: Geometrical Calculations

BY D. J. M. BEVAN* AND S. E. LAWTON

School of Physical Sciences, The Flinders University of South Australia, Bedford Park, South Australia 5042, *Australia*

(*Received* 6 *March* 1985; *accepted* 23 *July* 1985)

Abstract

The known structures of $Na_7Zr_6F_{31}$, KY_3F_{10} and tveitite ($Ca_{14}Y_5F_{43}$) have been modelled with clusters of six octahedrally arranged, cation-centred, Archimedian square antiprisms which share corners to generate a cuboctahedral cavity at the centre. This cluster, M_6X_{36}, has point symmetry $m3m$. The anion coordinates calculated from these polyhedral models are compared with observed values derived from X-ray data. Overall the polyhedral models are considered to be good approximations to the real structures.

Introduction

Aléonard, Le Fur, Pontonnier, Gorius & Roux (1978) first discussed the so-called fluorite-related structures of certain mixed alkali and rare-earth fluorides as a group. They defined 'fluorite-related' rather generally to mean the existence in a structure of layers of close-packed cations stacked one upon the other in no particular sequence: in fluorite itself, of course, the stacking sequence is *ABC*. It was clear from their work that a fundamental step in going from the fluorite structure to many superstructures was the conversion of MX_8 cubes to square antiprisms, six of which then shared edges to enclose an X_8 cube, just as six MX_8 cubes do in fluorite itself; both types of isolated cluster have contents M_6X_{32}.

Bevan, Greis & Strähle (1980) proposed another structural principle for *strictly* fluorite-related superstructures (in the sense that the close-packed layer stacking sequence is always *ABC*) in which six MX_8 square antiprisms share *corners* to generate an enclosed X_{12} cuboctahedron, giving rise to a cluster M_6X_{36} (or M_6X_{37} if an additional anion occupies the cavity within the cuboctahedron). Their paper contains photographs of polyhedral models of two known structures, $Na_7Zr_6F_{31}$ (Burns, Ellison & Levy, 1968) and tveitite, $Ca_{14}Y_5F_{43}$ (Bevan, Strähle & Greis, 1982). We were interested to determine just how well such models describe the actual structures, and to this end we have calculated anion coordinates from the models for comparison with those obtained experimentally. Only three structures are discussed here, $Na_7Zr_6F_{31}$, tveitite and KY_3F_{10} (Pierce & Hong, 1973), but the method is generally applicable.

$Na_7Zr_6F_{31}$

This compound is rhombohedral, space group $R\bar{3}$, with hexagonal unit-cell dimensions $a = 14{\cdot}1561\ (7)$, $c = 9{\cdot}579\ (7)$ Å. The relationship of this cell to that of the fluorite structure is given by

$$\begin{pmatrix} a_h \\ b_h \\ c_h \end{pmatrix} = \begin{pmatrix} 2{\cdot}00 & -1{\cdot}50 & -0{\cdot}50 \\ -0.50 & 2.00 & -1.50 \\ 1.00 & 1.00 & 1.00 \end{pmatrix} \begin{pmatrix} a_F \\ b_F \\ c_F \end{pmatrix}. \quad (1)$$

Zr_6F_{37} clusters are centred on lattice points, and each ZrF_8 square antiprism in a cluster shares one edge

* To whom all correspondence should be addressed.

0108-7681/86/010055-04$01.50

Table 1. *Calculated coordinates of the eight vertices of a square antiprism*

	Coordinates in terms of polyhedral edge **a**			Coordinates in terms of cubic unit cell *C*			Coordinates in terms of cubic unit cell *F*		
Vertex	*x*	*y*	*z*	*x*	*y*	*z*	*x*	*y*	*z*
1	1·548a	0·500a	0·500a	1·000	0·323	0·323	0·774	0·250	0·250
2	0·707a	0·707a	0·000a	0·457	0·457	0·000	0·354	0·354	0·000
3	1·548a	0·500a	−0·500a	1·000	0·323	−0·323	0·774	0·250	−0·250
4	0·707a	0·000a	−0·707a	0·457	0·000	−0·457	0·354	0·000	−0·354
5	1·548a	−0·500a	−0.500a	1·000	−0.323	−0.323	0·774	−0.250	−0.250
6	0·707a	−0.707a	0·000a	0·457	−0.457	0·000	0·354	−0·354	0·000
7	1·548a	−0·500a	0·500a	1·000	−0·323	0·323	0·774	−0·250	0·250
8	0·707a	0·000a	0·707a	0·457	0·000	0·457	0·354	0·000	0·354

with a square antiprism of an adjacent cluster [see Fig. 4 of Bevan *et al.* (1980)]. *All* the anions of the structure are generated by this arrangement of clusters.

KY_3F_{10}

This compound is cubic, space group $Fm3m$, with $a = 11{\cdot}536\,(4)$ Å: its unit cell is a $2\times2\times2$ supercell of fluorite. Y_6F_{36} clusters are centred on $\frac{1}{2}, \frac{1}{2}, \frac{1}{2}$ *etc.*, and each YF_8 square antiprism of a cluster shares all four edges of its outer square face with like edges from adjacent clusters. Again, *all* the anions of the structure are generated by this cluster array.

Models of both these structures have the correct symmetry.

$Ca_{14}Y_5F_{43}$, *tveitite*

This is another rhombohedral compound, space group $R\bar{3}$, with hexagonal unit-cell dimensions $a = 16{\cdot}6920\,(9)$, $c = 9{\cdot}6664\,(8)$ Å. The unit-cell relationship between tveitite and fluorite is given by

$$\begin{pmatrix} a_h \\ b_h \\ c_h \end{pmatrix} = \begin{pmatrix} 2{\cdot}50 & -1{\cdot}00 & -1{\cdot}50 \\ -1{\cdot}50 & 2{\cdot}50 & -1{\cdot}00 \\ 1{\cdot}00 & 1{\cdot}00 & 1{\cdot}00 \end{pmatrix} \begin{pmatrix} a_F \\ b_F \\ c_F \end{pmatrix}. \quad (2)$$

$(CaY_5)F_{37}$ clusters are centred on lattice points, the two types of cation being randomly distributed over the six square-antiprism centres. These clusters in the tveitite structure are not, however, linked directly by edge sharing [see Fig. 3 of Bevan *et al.* (1980)], but are connected through pairs of edge-sharing F_8 cubes, each of which is joined by face sharing to square antiprisms of two separate clusters. With discrete clusters the cluster anions themselves do not constitute all the anions of the structure, and one of the seven 18(f) anion sites in this structure stems from the linking cubes. It transpires that this model does not quite have $R\bar{3}$ symmetry, although it is very close.

Calculation of coordinates of polyhedral vertices in models

Fig. 1 depicts a cluster, viewed along a threefold axis, of six ideal square antiprisms with edge **a** sharing corners to enclose an undistorted cuboctahedron. The point symmetry of such a cluster is $m3m$. We choose an origin at the centre of the cuboctahedron and construct an orthogonal axial set as shown. These axes are also those of the fluorite structure. Table 1 lists for completeness the calculated coordinates of all eight vertices of one square antiprism (see Fig. 1) and we therefore have from symmetry considerations the coordinates of all cluster vertices. Table 1 also gives fractional coordinates in terms of two cells, one designated *C*, with unit vectors equal to 1·548**a** (this is the vector from the origin to the centre of an outer square face of a square antiprism), and another, designated *F*, with unit vectors equal to 2**a**, corresponding to the fluorite unit cell of edge-sharing cubes of edge **a**.

We now proceed to calculate coordinates of cluster vertices in terms of the supercells. Use of the formal relationship between supercell and subcell assumes no distortion from the cubic metric of the latter (and therefore takes no account of any discrepancy in size between the square-antiprism cluster and the analogous cube cluster, M_6X_{32}): this leads to certain conflicting results in the cases of $Na_7Zr_6F_{31}$ and KY_3F_{10}. In particular, some non-identical vertices which are crystallographically equivalent by virtue of edge-sharing between clusters do not calculate as such. For tveitite, where the clusters are discrete, this problem does not arise; however, not all anion coordinates can be calculated.

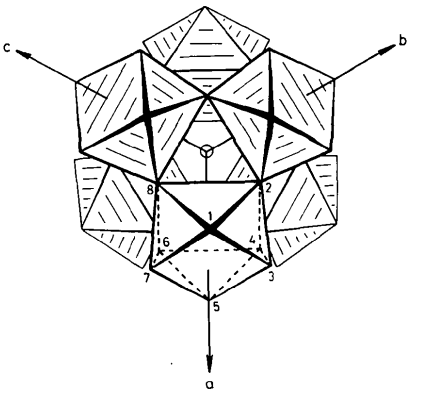

Fig. 1. A schematic drawing of the M_6F_{37} cluster, showing the orthogonal axes: the labelled vertices represent those used in the calculations.

Table 2. *Calculated and experimental coordinates for* $Na_7Zr_6F_{31}$

		Experimental coordinates*			Calculated coordinates (from model)		
	Vertex	*x*	*y*	*z*	*x*	*y*	*z*
F(1)	3, 5	0·3558	0·1114	0·0917	0·3589	0·1047	0·0872
F(2)	1	0·1835	0·0554	0·3944	0·1837	0·0536	0·4052
F(3)	7	0·2735	0·3706	0·4243	0·2627	0·3613	0·4205
F(4)	4, 6	0·2088	0·1585	0·0017	0·2118	0·1601	0·0000
F(5)	2, 8	0·2432	0·5417	0·4416	0·2455	0·5428	0·4418
F(6)	—	0·0000	0·0000	0·0526	0·0000	0·0000	0·0000

* From Burns, Ellison & Levy (1968).

Table 3. *Calculated and experimental coordinates for* KY_3F_{10}

		Experimental coordinates*			Calculated coordinates (from model)		
	Vertex	*x*	*y*	*z*	*x*	*y*	*z*
F(1)	2, 4, 6, 8	0·000	0·1647	0·1647	0·000	0·1726	0·1726
F(2)	1, 3, 5, 7	0·6081	0·6081	0·6081	0·6221	0·6221	0·6221

* From Pierce & Hong (1973), but with their origin shifted by $\frac{1}{2}, \frac{1}{2}, \frac{1}{2}$ to conform with ours.

An alternative procedure is to work directly from the model. The calculations are then entirely self-consistent provided that the clusters share edges directly in some way so as to form a three-dimensional network.

The supercell parameters with respect to the cubic unit cell C (see Table 1) are determined by tracing paths from the origin to other appropriate lattice points. As a first stage we determine the coordinates of these lattice points in terms of the polyhedral edge **a**, from which we can write (for $Na_7Zr_6F_{31}$)

$$\begin{aligned} a_h &= (4{\cdot}096\mathbf{a}, \quad -3{\cdot}096\mathbf{a}, \quad -1{\cdot}000\mathbf{a}) - (0,0,0) \\ b_h &= (-1{\cdot}000\mathbf{a}, \quad 4{\cdot}096\mathbf{a}, \quad -3{\cdot}096\mathbf{a}) - (0,0,0). \\ c_h &= (2{\cdot}096\mathbf{a}, \quad 2{\cdot}096\mathbf{a}, \quad 2{\cdot}096\mathbf{a}) - (0,0,0) \end{aligned} \quad (3)$$

Comparison of the half values of these coordinates with the elements of the 3×3 matrix in equation (1) immediately reveals the small discrepancy in size between the square-antiprism (M_6X_{36}) and cube (M_6X_{32}) clusters.

The relationship between the supercell and the cubic cell C is now written as

$$\begin{pmatrix} a_h \\ b_h \\ c_h \end{pmatrix} = \begin{pmatrix} 2{\cdot}6460 & -2{\cdot}0000 & -0{\cdot}6460 \\ -0{\cdot}6460 & 2{\cdot}6460 & -2{\cdot}0000 \\ 1{\cdot}3540 & 1{\cdot}3540 & 1{\cdot}3540 \end{pmatrix} \begin{pmatrix} a_c \\ b_c \\ c_c \end{pmatrix}. \quad (4)$$

We then proceed conventionally to calculate coordinates of the cluster vertices for the hexagonal cell. These coordinates are listed in Table 2, together with the experimental coordinates for comparison. Table 3 contains the data for KY_3F_{10}, obtained in the same way.

For tveitite the M_6X_{37} clusters are discrete, and the model [see Fig. 3 of Bevan *et al.* (1980)] makes use of empty cubes to achieve connectivity. The primary M_6X_{37} cluster is expanded by the addition of six such cubes, one for each square antiprism and joined to it by face sharing: these larger clusters share edges to fill space. Calculations such as the above based on this model now lead to some minor discrepancies, as

Table 4. *Calculated and experimental coordinates for tveitite* ($Ca_{14}Y_5F_{43}$)

					Calculated coordinates					
					From formal subcell/ supercell relationship					
		Experimental coordinates*						From model		
	Vertex	*x*	*y*	*z*	*x*	*y*	*z*	*x*	*y*	*z*
F(1)	4, 6	0·1958	0·0831	0·0040	0·1861	0·0744	0·0000	0·1827	0·0734	0·0000
F(2)	2, 8	0·1102	0·0975	0·2349	0·0993	0·0868	0·2357	0·0973	0·0853	0·2357
F(3)	1	0·0190	0·1495	0·4146	0·0184	0·1471	0·4246	0·0178	0·1444	0·4247
F(4)	3	0·2702	0·1024	0·2573	0·2690	0·1044	0·2580	0·2642	0·1030	0·2580
F(5)	7	0·1576	0·2686	0·2515	0·1587	0·2698	0·2580	0·1554	0·2650	0·2580
	†*D*							0·1610	0·2640	0·2420
F(6)	5	0·0324	0·2842	0·0971	0·0359	0·2874	0·0913	0·0346	0·2818	0·0913
	†*B*							0·0344	0·2818	0·0914
F(7)	†*A*	0·2955	0·3838	0·0744	—	—	—	0·2986	0·3847	0·0754
	†*C*							0·2987	0·3848	0·0753
F(8)	—	0·0000	0·0000	0·0600	0·0000	0·0000	0·0000	0·0000	0·0000	0·0000

* From Bevan, Strähle & Greis (1982).

† Vertices *A*, *B*, *C* and *D* refer to the other four corners of an empty cube sharing the face (1, 3, 5, 7) of a cluster square antiprism (see text).

Table 5. *Cation coordinates for* $Na_7Zr_6F_{31}$

				Calculated for equivalent supercell of ideal fluorite					
	Observed						Calculated from polyhedral model		
Na(1)	0·0792,	0·3040,	0·4926	0·0769,	0·3077,	0·5000	—	—	—
Na(2)	0,	0,	$\frac{1}{2}$	0,	0,	$\frac{1}{2}$	0,	0,	$\frac{1}{2}$
Zr	0·1896,	0·0515,	0·1790	0·1795,	0·0513,	0·1667	0·1976,	0·0576,	0·1793

shown in Table 4, which arise from the fact that the model does not quite have $R\bar{3}$ symmetry.

So far we have considered only the anions of the structure, because it is these which are displaced significantly from ideal fluorite sites. The cations suffer only minor displacements from the ideal f.c.c. positions. However, only those cation sites in the models which can, to a good approximation, be centred within *regular* polyhedra (*e.g.* square antiprisms, cubes) can be calculated. Thus, for example, the coordinates of the 18(*f*) Zr site in $Na_7Zr_6F_{31}$ are calculable, but not for the 18(*f*) Na(1) site. Comparative data for $Na_7Zr_6F_{31}$ are shown in Table 5.

Overall, then, for the three structures discussed, the calculations are in good agreement with observations, and we consider the polyhedral models to be good approximations to the real structures. In a subsequent paper we shall show how such calculations on a polyhedral model of a *postulated* structure have been used, with *X*-ray powder data, as the starting point of a successful refinement.

We thank Dr H. J. Rossell and Professor B. Abrahamson for much helpful discussion.

We also acknowledge the provision of financial assistance by the Australian Research Grants Scheme.

References

ALÉONARD, S., LE FUR, Y., PONTONNIER, L., GORIUS, M. F. & ROUX, M. T. (1978). *Ann. Chim.* **3**, 417-427.

BEVAN, D. J. M., GREIS, O. & STRÄHLE, J. (1980). *Acta Cryst.* A**36**, 889-890.

BEVAN, D. J. M., STRÄHLE, J. & GREIS, O. (1982). *J. Solid State Chem.* **44**, 75-81.

BURNS, J. H., ELLISON, R. D. & LEVY, H. A. (1968). *Acta Cryst.* B**24**, 230-237.

PIERCE, J. W. & HONG, H. Y. P. (1973). *Proceedings of the Tenth Rare-Earth Research Conference*, edited by C. J. KEVANE, pp. 527-537. US Atomic Energy Commission, Technical Information Center.

Acta Cryst. (1986). B**42**, 58-61

Textures in Natural Pyrolusite, β-MnO_2, Examined by 1 MV HRTEM

BY N. YAMADA AND M. OHMASA

Institute of Materials Science, University of Tsukuba, Ibaraki 305, *Japan*

AND S. HORIUCHI

National Institute for Research in Inorganic Materials, Ibaraki 305, *Japan*

(*Received* 1 *July* 1985; *accepted* 23 *August* 1985)

Abstract

Textures in natural pyrolusite have been studied by 1 MV high-resolution transmission electron microscopy (HRTEM). The structure is mainly of the rutile type with many lamellae of a different structure. Most of the lamellae, being parallel to each other, are perpendicular to one of the tetragonal *a* axes of the pyrolusite and are separated by about 9 nm. Their structure was inferred to be similar to that of ramsdellite. There are many holes located along the lamellae. The cross section of some holes is rhombic and their edges are almost parallel to ⟨110⟩; they vary in size from ten to several hundred nm^2. The holes must be produced in the process of the phase transformation of manganite into pyrolusite.

Introduction

The structure unit in manganese oxides and hydroxide oxides is an MnO_6 octahedron, which shares opposite edges with adjoining octahedra to form an infinite chain. The period of the chain is 0·28 nm. Double or triple chains are formed when two or three parallel chains are combined with each other by sharing edges of the constituent octahedra. Many varieties of framework structures have so far been found for manganese oxides which are built of single or multiple chains by sharing their corners (Wells, 1975).

There are three reasons why the study of the phase and structure relation among these compounds is difficult: (i) many polymorphs with different combinations of chains have been found in these compounds, but the stability relation among them is still not clear; (ii) various kinds of cations can be easily accommodated in the interstices of the framework and give a complex formula; in this case some of the Mn^{4+} in the framework are replaced by Mn^{3+} or other cations with smaller charges; and (iii) many of these compounds are often found or synthesized as brittle, poorly crystallized materials. (iii) is the principal reason why these materials have not yet been fully characterized crystallographically. Consequently,

0108-7681/86/010058-04$01.50